

## Article

# Design and Fabrication of $\alpha$ -MnO<sub>2</sub>-Nanorods-Modified Glassy-Carbon-Electrode-Based Serotonin Sensor

Mohd Quasim Khan <sup>1,†</sup>, Rais Ahmad Khan <sup>2</sup>, Ali Alsalmeh <sup>2,\*</sup>, Khursheed Ahmad <sup>3,†</sup>  
and Haekyoung Kim <sup>3,\*</sup>

<sup>1</sup> Department of Chemistry, M.M.D. College, Moradabad, M.J.P. Rohilkhand University, Bareilly 244001, UP, India

<sup>2</sup> Department of Chemistry, College of Science, King Saud University, Riyadh 11451, Saudi Arabia

<sup>3</sup> School of Materials Science and Engineering, Yeungnam University, Gyeongsan 38541, Korea

\* Correspondence: aalsalmeh@ksu.edu.sa (A.A.); hkkim@ynu.ac.kr (H.K.)

† These authors contributed equally to this work.

**Abstract:** Serotonin is a very important monoamine neurotransmitter, which takes part in biological and psychological processes. In the present scenario, design and fabrication of a serotonin electrochemical sensor is of great significance. In this study, we have synthesized  $\alpha$ -MnO<sub>2</sub> via a hydrothermal synthesis method using potassium permanganate as a precursor. The physiochemical properties, such as structural and phase-purity of the prepared  $\alpha$ -MnO<sub>2</sub>, were investigated by various characterization techniques and methods (powder X-ray diffraction, scanning electron microscopy, and energy-dispersive X-ray spectroscopy). Furthermore, the serotonin sensor was fabricated using  $\alpha$ -MnO<sub>2</sub> as an electrode modifier or electro-catalyst. The bare glassy carbon electrode (GCE) was adopted as a working substrate, and its active carbon surface was modified with the synthesized  $\alpha$ -MnO<sub>2</sub>. This modified GCE ( $\alpha$ -MnO<sub>2</sub>/GCE = MGCE) was explored as a serotonin sensor. The electrochemical investigations showed that the MGCE has excellent electro-catalytic properties towards determination of serotonin. The MGCE exhibits an excellent detection limit (DL) of 0.14  $\mu$ M, along with good sensitivity of 2.41  $\mu$ A $\mu$ M<sup>-1</sup> cm<sup>-2</sup>. The MGCE also demonstrated excellent selectivity for determination of serotonin in the presence of various electro-active/interfering molecules. The MGCE also exhibits good cyclic repeatability, stability, and storage stability.

**Keywords:**  $\alpha$ -MnO<sub>2</sub>/GCE; serotonin; sensor; electrochemistry



**Citation:** Khan, M.Q.; Khan, R.A.; Alsalmeh, A.; Ahmad, K.; Kim, H. Design and Fabrication of  $\alpha$ -MnO<sub>2</sub>-Nanorods-Modified Glassy-Carbon-Electrode-Based Serotonin Sensor. *Biosensors* **2022**, *12*, 849. <https://doi.org/10.3390/bios12100849>

Received: 11 September 2022

Accepted: 6 October 2022

Published: 9 October 2022

**Publisher's Note:** MDPI stays neutral with regard to jurisdictional claims in published maps and institutional affiliations.



**Copyright:** © 2022 by the authors. Licensee MDPI, Basel, Switzerland. This article is an open access article distributed under the terms and conditions of the Creative Commons Attribution (CC BY) license (<https://creativecommons.org/licenses/by/4.0/>).

## 1. Introduction

Serotonin, which is a monoamine neurotransmitter, plays a significant role in biological, physical, and psychological processes, such as appetite control, sleep pattern, sexual activity, and aggression [1,2]. The amount of serotonin in the human body should be controlled, and the normal range of serotonin in serum lies between 0.57 and 2.0  $\mu$ M, whereas its normal amount in urine is considered in the range of 0.295–0.687  $\mu$ M [3]. Serotonin has the potential to control and maintain all vital activities [4]. Presence of a low level of serotonin may cause various diseases, such as sexual dysfunction, Alzheimer's disease, depression, and Parkinson's disease [5,6]. Thus, it is of great significance to design and develop a highly precise, rapid, and sensitive technique or method for detection of serotonin level in human bio-fluids [7]. This can be helpful to diagnose diseases linked to serotonin. In previous years, various methods and techniques, such as high-performance liquid chromatography, capillary electrophoresis, enzyme immunoassay, fluorescence spectrophotometry, and mass spectrometry, were used as sensing platforms for determination of serotonin [8–12]. Although the above conventional methods were widely used for determination of serotonin, including other analytes, there are some limitations, such as complicated pretreatment processes, being time-consuming, and requiring expensive instruments, including well-trained operators [13]. These factors restrict rapid detection of

serotonin with frequent testing, and it will be of great importance to discover or develop other alternative methods for rapid determination of serotonin [14]. Electrochemistry-based analytical or electrochemical methods have gained enormous attention because of their simple process, fast response/detection, ease of operation, and selectivity [15–19]. In addition, electrochemical techniques offer highly sensitive analysis with a cost-effective miniaturized platform [20]. Previously, a number of electrochemistry-based sensors were developed for sensing of serotonin. Indeed, various electrode materials, such as zinc oxide, nickel hydroxide ( $\text{Ni(OH)}_2$ ), carbon nanotubes, reduced graphene oxide, tungsten trioxide, gold nanoparticles, polymers, zirconium oxide ( $\text{ZrO}_2$ ), copper oxide, cobalt oxide, iron oxide, carbon nitride, and their hybrid composites, have been explored as serotonin sensing material [13,21–28]. However, there is still a need to develop a cost-effective and highly sensitive selective serotonin sensor.

Manganese oxide ( $\alpha\text{-MnO}_2$ ) has gained enormous interest in the scientific community because of its excellent electro-catalytic properties, better inherent molecular adsorption ability, cost-effectiveness, excellent ion-exchange capability, natural abundance, and non-toxicity [29]. Further,  $\alpha\text{-MnO}_2$  has been widely explored in a variety of applications, such as sensors, dye-sensitized solar cells, energy storage, batteries, catalysis, and dye degradation [30–35]. Previous reports showed that  $\alpha\text{-MnO}_2$  is a potential candidate for fabrication of electrochemical sensors [30]. Herein, we have developed a serotonin sensor using  $\alpha\text{-MnO}_2$  as electrode material. The  $\alpha\text{-MnO}_2$ -based serotonin sensor exhibits excellent performance.

## 2. Materials and Methods

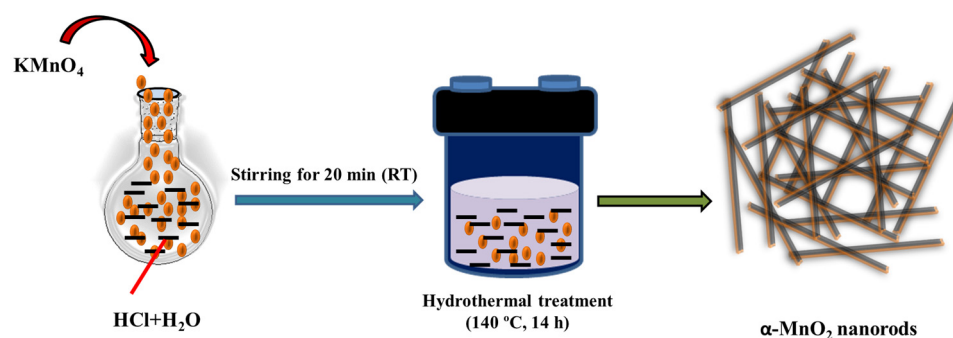
### 2.1. Chemicals

Potassium permanganate ( $\text{KMnO}_4$ ), serotonin, and hydrochloric acid ( $\text{HCl}$ , 37%) were purchased from Merck. Ascorbic acid and glucose were purchased from Sigma. Nafion was purchased from Sigma. Phosphate buffer saline solutions (PBS) were purchased from Loba. Uric acid was purchased from Alfa Aesar. Dopamine was purchased from TCI. Urea was purchased from Fischer Scientific.

### 2.2. Synthesis of $\alpha\text{-MnO}_2$

The  $\alpha\text{-MnO}_2$  was synthesized according to procedures reported elsewhere with some minor modifications [31]. In brief, 3 mmol of  $\text{KMnO}_4$  was dissolved in 25 mL of deionized (D.I.) water and 7.5 mmol of  $\text{HCl}$  was added.

This solution was stirred for 20 min at room temperature (RT), and transparent purple colored solution was obtained. This purple-colored solution was poured in to the Teflon-lined (capacity 50 mL) stainless steel autoclave reactor, which was heated at 140 °C for 12 h (Scheme 1). The precipitate was collected by centrifugation and washed with distilled water several times and dried at 70 °C overnight in vacuum oven.



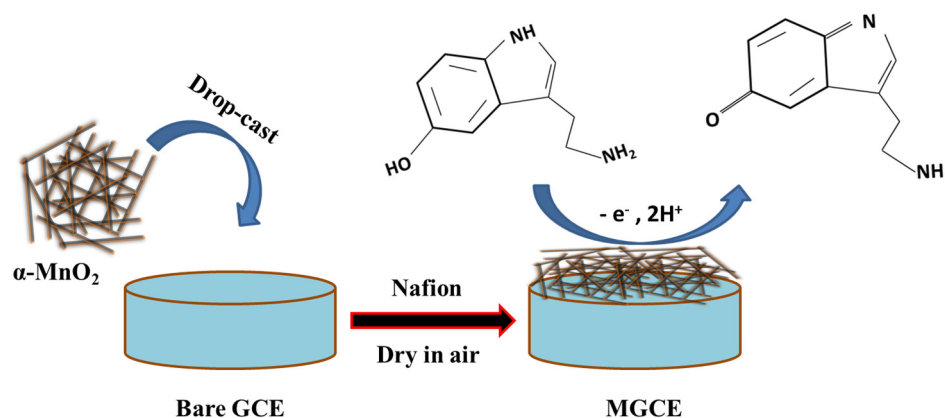
**Scheme 1.** Pictorial representation for synthesis of  $\alpha\text{-MnO}_2$ .

### 2.3. Instrumental Characterization

The phase-purity and confirmation of successful formation of  $\alpha$ -MnO<sub>2</sub> were authenticated by various characterization techniques. In this connection, powder X-ray diffraction (PXRD) pattern of the hydrothermally synthesized  $\alpha$ -MnO<sub>2</sub> was collected on Rigaku, Japan (RINT 2500 V XRD Instrument) with Cu K $\alpha$  irradiation at two-Theta range of 10–80°. The structural phase of the prepared  $\alpha$ -MnO<sub>2</sub> was identified using PXRD investigations. The morphological characteristic of the prepared  $\alpha$ -MnO<sub>2</sub> was examined by utilizing scanning electron microscopy (SEM). The SEM images of the prepared  $\alpha$ -MnO<sub>2</sub> were collected on S-4800 (Hitachi) instrument. The elemental composition of the hydrothermally prepared  $\alpha$ -MnO<sub>2</sub> was investigated by utilizing energy-dispersive X-ray spectroscopy (EDS). The EDS spectrum of the hydrothermally prepared  $\alpha$ -MnO<sub>2</sub> was collected on Horiba EDS instrument. Electrochemical investigations were carried out using CH Instrument (silver/silver electrode was used as reference electrode, while platinum wire used as counter electrode). The bare glassy carbon electrode (BGCE) and  $\alpha$ -MnO<sub>2</sub>-modified GCE ( $\alpha$ -MnO<sub>2</sub>/GCE = MGCE) was used as working electrode.

### 2.4. Fabrication of Working Electrode

The  $\alpha$ -MnO<sub>2</sub> ink was prepared by dispersing 2.5 mg of  $\alpha$ -MnO<sub>2</sub> in 2 mL of distilled water (having 0.1% nafion) using ultrasonication for 30 min. Nafion was used as binder to increase the adhesiveness of the  $\alpha$ -MnO<sub>2</sub> on GCE surface. Further, 8.5  $\mu$ L of the prepared ink was drop-casted on to the carbon surface of the GCE and dried in air for 4 h (Scheme 2).



**Scheme 2.** Pictorial representation for fabrication and working mechanism of MGCE towards serotonin sensing.

## 3. Results

### 3.1. Physiochemical Properties of $\alpha$ -MnO<sub>2</sub>

The collected PXRD data of the prepared  $\alpha$ -MnO<sub>2</sub> are presented in Figure 1. The PXRD pattern revealed the presence of several diffraction peaks at ~12.72, 18.13, 28.75, 37.70, 42.01, 49.96, 56.26, 60.12, 65.44, 69.41, and 72.96°. These diffraction peaks of 12.72, 18.13, 28.75, 37.70, 42.01, 49.96, 56.26, 60.12, 65.44, 69.41, and 72.96° can be assigned to the well-defined (110), (200), (310), (211), (301), (411), (600), (521), (002), (541), and (312) diffraction planes of  $\alpha$ -MnO<sub>2</sub>. The obtained PXRD pattern of the hydrothermally synthesized  $\alpha$ -MnO<sub>2</sub> was found to be in good agreement with previous JCPDS card number 044-0141. The PXRD pattern of the prepared  $\alpha$ -MnO<sub>2</sub> does not show any other diffraction peak for impurity, which suggests successful formation of  $\alpha$ -MnO<sub>2</sub> with decent phase-purity. The crystallite size of the prepared  $\alpha$ -MnO<sub>2</sub> was determined by employing the Scherrer equation, as provided below:

$$D = \frac{K\lambda}{\beta \cos \theta} \quad (1)$$

(In the above equation 1,  $K$  = Scherrer constant, which is equal to 0.9,  $D$  is the average crystallite-size ( $\text{\AA}$ ), whereas  $\lambda$  is the X-ray wavelength (0.154 nm), and  $\theta$  is the diffraction-angle;  $\beta$  represents full width at half-maximum (FWHM) of the observed peak). The crystallite size of the  $\alpha\text{-MnO}_2$  was found to be  $\sim 31.4$  nm using the Scherrer equation. Our obtained PXRD results for the prepared  $\alpha\text{-MnO}_2$  are in good agreement with previously published literature and suggest successful formation of  $\alpha\text{-MnO}_2$  with good phase-purity.

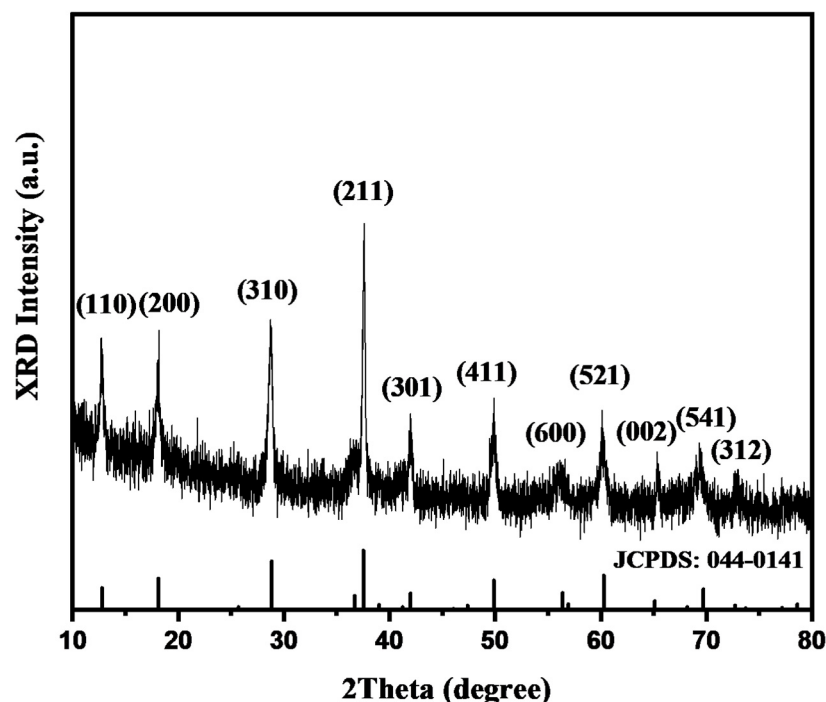


Figure 1. PXRD pattern of the hydrothermally prepared  $\alpha\text{-MnO}_2$ .

It has been determined from the reported studies that surface morphology of electrode materials plays a significant role and influences the electrochemical performance of the developed sensors. In this regard, it is necessary to investigate the morphological characteristics of the prepared  $\alpha\text{-MnO}_2$  material. The obtained SEM pictures of the synthesized  $\alpha\text{-MnO}_2$  at different magnifications have been displayed in Figure 2a–d. The SEM results indicate that hydrothermally prepared  $\alpha\text{-MnO}_2$  comprised a rod-like surface. Therefore, it is clear that  $\alpha\text{-MnO}_2$  has been successfully obtained with a rod-like surface morphology of a nanometer in size. To further verify the phase-purity of the hydrothermally prepared  $\alpha\text{-MnO}_2$ , it is necessary to examine the elemental composition of the hydrothermally prepared  $\alpha\text{-MnO}_2$ . Hence, we have examined the elemental composition of the hydrothermally prepared  $\alpha\text{-MnO}_2$ . The EDS results of the  $\alpha\text{-MnO}_2$  are presented in Figure 3a–d. The EDS electron image of the hydrothermally prepared  $\alpha\text{-MnO}_2$  is presented in Figure 3a, while the EDS spectrum of the  $\alpha\text{-MnO}_2$  is depicted in Figure 3b. The EDS spectrum of the  $\alpha\text{-MnO}_2$  exhibits the presence of Mn and O elements, which indicates that  $\alpha\text{-MnO}_2$  has been successfully prepared.

The EDS mapping image of the Mn and O elements has been displayed in Figures 3c and 3d, respectively. The atomic percentage of the Mn and O elements was found to be 33.46 and 66.54%, whereas the weight percentage of the Mn and O elements was found to be 64.13 and 35.87%, respectively.

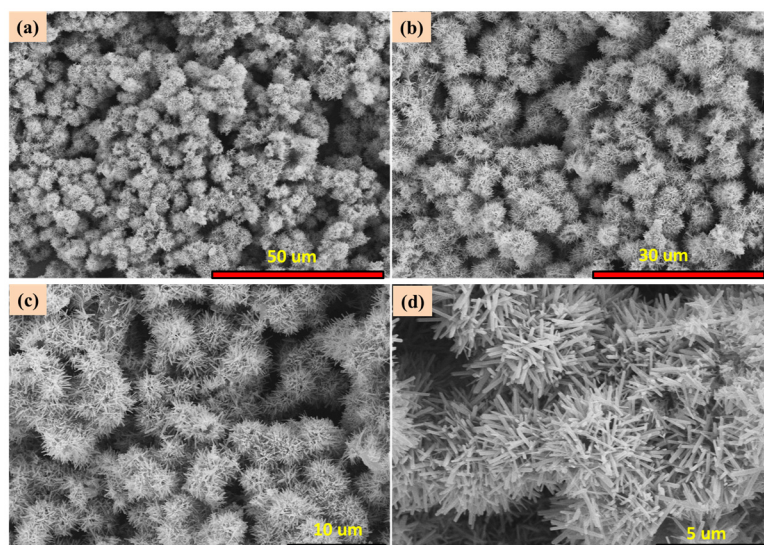


Figure 2. SEM pictures of the prepared  $\alpha$ -MnO<sub>2</sub> at different magnifications (a–d).

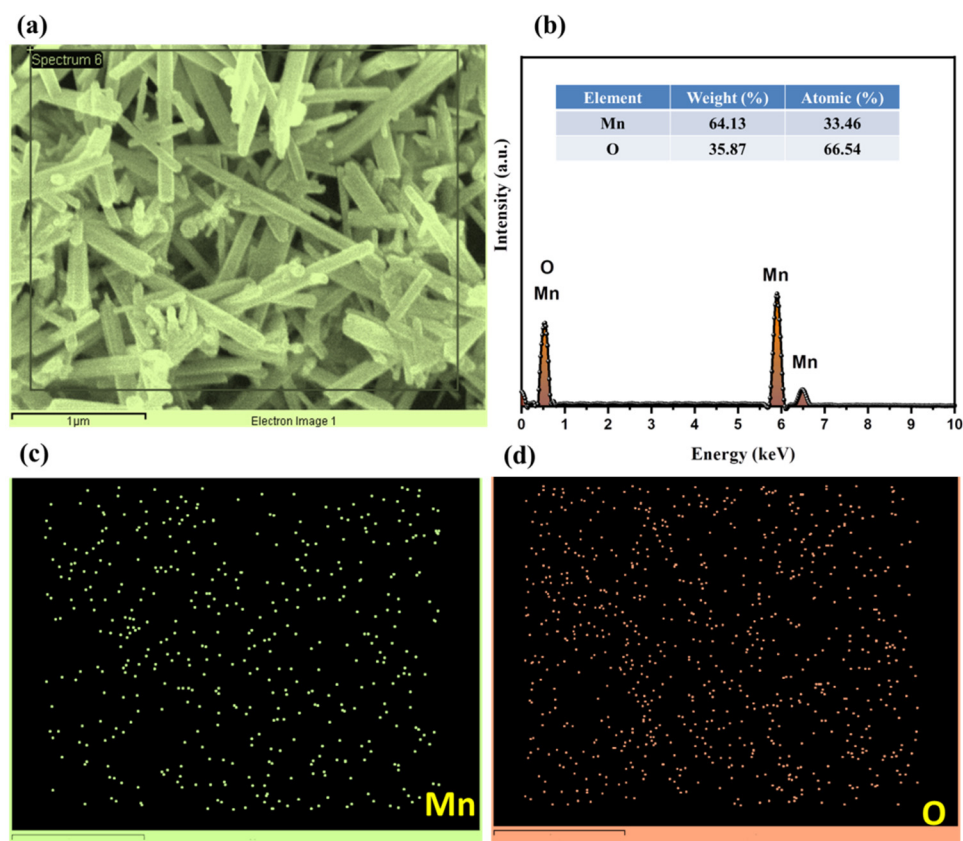


Figure 3. EDX electron image (a), EDX spectrum (b), and mapping images (c,d) of the prepared  $\alpha$ -MnO<sub>2</sub>.

No other element was observed in the EDS spectrum of the hydrothermally prepared  $\alpha$ -MnO<sub>2</sub>. This suggests that  $\alpha$ -MnO<sub>2</sub> has good phase-purity. The above overall PXRD, SEM, and EDX results are consistent with previous reports and authenticated the formation of  $\alpha$ -MnO<sub>2</sub> with a nanorods-like surface morphology. According to the previous literature [31], electrode materials with rod-like surface morphology are the desirable materials for construction of electrochemical sensors. The rod-like surface of the electrode materials

provides better bath and fast electron transportation. Thus, we have fabricated a serotonin electrochemical sensor using GCE as a working substrate and  $\alpha$ -MnO<sub>2</sub> as electrode material.

### 3.2. Electrochemical Properties of MGCE

The electrochemical activity of the BGCE and MGCE were determined using cyclic voltammetry (CV). The CVs of the BGCE and MGCE were taken in presence and absence of 2  $\mu$ M serotonin in 0.1 M PBS of pH 7.0 at an applied scan rate of 50 mV/s. The collected CVs of the BGCE and MGCE in absence and presence of 2  $\mu$ M serotonin in 0.1 M PBS of pH 7.0 at an applied scan rate of 50 mV/s are displayed in Figure 4. The BGCE showed poor electro-catalytic activity, whereas MGCE showed slightly enhanced electro-catalytic activity in absence of serotonin (Figure 4). The BGCE exhibited a current response of 0.77  $\mu$ A for oxidation of 2  $\mu$ M serotonin in 0.1 M PBS of pH 7.0 at an applied scan rate of 50 mV/s. Conversely, MGCE showed an improved current response of 1.41  $\mu$ A for the oxidation of 2  $\mu$ M serotonin in 0.1 M PBS of pH 7.0 at an applied scan rate of 50 mV/s (Figure 4). The CVs observations revealed that MGCE has higher current response compared to BGCE (Figure 4). This improved current response indicates successful deposition of  $\alpha$ -MnO<sub>2</sub> on GCE surface. In addition, the improved electro-catalytic activity of the MGCE can be attributed to the presence of good electrochemical features of  $\alpha$ -MnO<sub>2</sub>. We selected MGCE as the serotonin sensor for further electrochemical investigations.

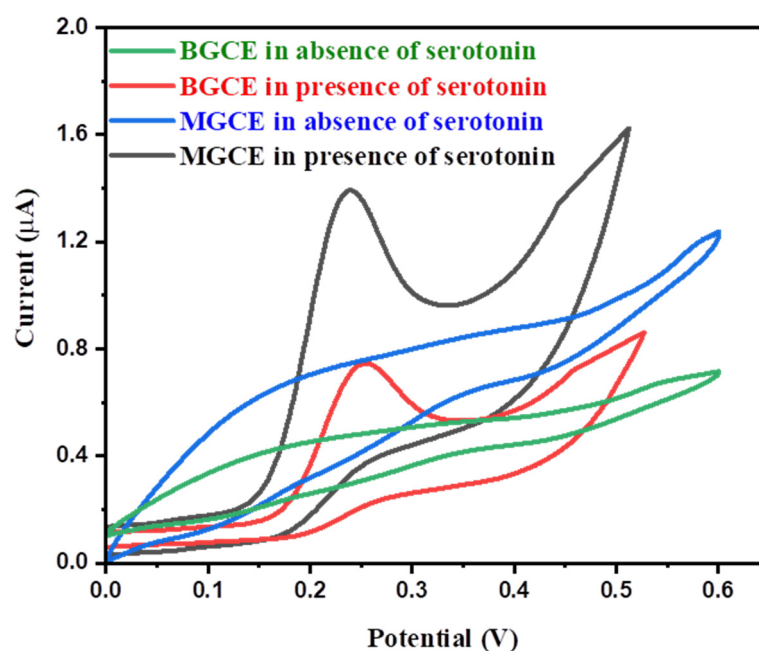


**Figure 4.** CVs of BGCE and MGCE in absence and presence of 2  $\mu$ M serotonin in 0.1 M PBS (pH = 7.0) at scan rate of 50 mV/s.

The concentration of the analyte has the potential to affect the electrochemical performance of the fabricated electrochemical sensors. It has also been observed from the previous reports that the concentration of serotonin largely influences the electrochemical sensing performance of the constructed sensors. Thus, it is important to study the effect of concentration of serotonin on the electrochemical performance of the fabricated MGCE. Hence, we collected CVs of the MGCE in various concentrations of serotonin (2  $\mu$ M, 9  $\mu$ M, 16  $\mu$ M, 23  $\mu$ M, 30  $\mu$ M, 37  $\mu$ M, 45  $\mu$ M, 55  $\mu$ M, 70  $\mu$ M, and 80  $\mu$ M) in 0.1 M PBS (pH = 7.0) at an applied scan rate of 50 mV/s. The obtained CVs of the MGCE in various concentrations of serotonin (2  $\mu$ M, 9  $\mu$ M, 16  $\mu$ M, 23  $\mu$ M, 30  $\mu$ M, 37  $\mu$ M, 45  $\mu$ M, 55  $\mu$ M, 70  $\mu$ M, and 80  $\mu$ M) in 0.1 M PBS (pH = 7.0) at an applied scan rate of 50 mV/s are displayed in Figure 5a.

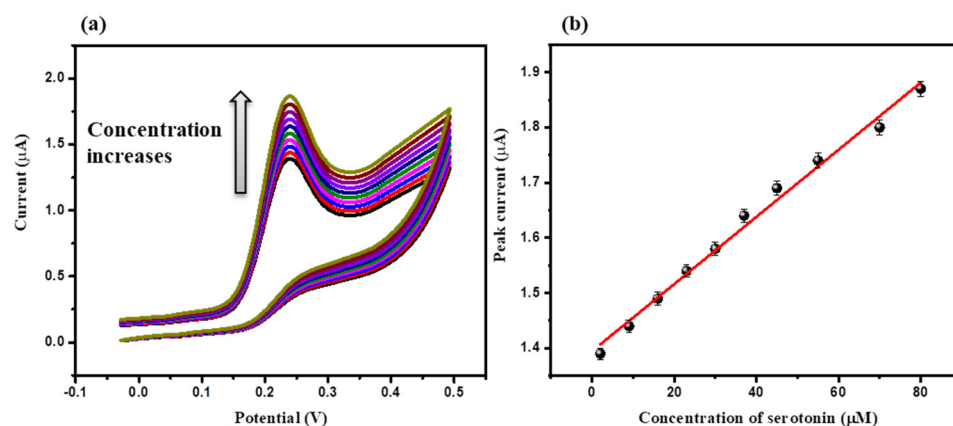


**Figure 5.** CVs (a) of MGCE in various concentrations (2  $\mu\text{M}$ , 9  $\mu\text{M}$ , 16  $\mu\text{M}$ , 23  $\mu\text{M}$ , 30  $\mu\text{M}$ , 37  $\mu\text{M}$ , 45  $\mu\text{M}$ , 55  $\mu\text{M}$ , 70  $\mu\text{M}$ , and 80  $\mu\text{M}$ ) of serotonin in 0.1 M PBS (pH = 7.0) at fixed scan rate of 50 mV/s. Calibration curve (b) between peak current response versus concentration of serotonin.

The observations showed that current response of the MGCE increases with increasing the concentration of serotonin from 2  $\mu\text{M}$  to 80  $\mu\text{M}$  (Figure 5a). This indicated that concentration of serotonin has a significant role on electrochemical activity of MGCE. The calibration curve between the peak current response of MGCE and serotonin concentration were plotted to ascertain the linear relation. The calibration curve of the peak current response of the MGCE versus concentration of serotonin is presented in Figure 5b. This calibration curve suggests that current response increases linearly with increasing concentration of serotonin (Figure 5b), with  $R^2 = 0.99$ .

The applied scan rate also plays an important role in electrochemical sensing investigations. We also studied the effect of various applied scan rates on the electrochemical performance of the MGCE at a fixed concentration. The CVs of the MGCE were taken in the presence of 2  $\mu\text{M}$  serotonin in 0.1 M PBS (pH = 7.0) at various applied scan rates (50, 75, 100, 125, 150, 175, 200, 225, 250, and 275 mV/s). The CVs results showed that the current response of the MGCE increases when the applied scan rate changes from 50 mV/s to 75 mV/s. Further investigations showed that current response increases while increasing the applied scan rate from 50 mV/s to 225 mV/s (Figure 6a). The calibration curve of the peak current response and square root of the applied scan rate is presented in Figure 6b, with an  $R^2$  value of 0.92. Further, we also plotted the calibration curve between the peak current response of the MGCE and applied scan rates. Figure 6c shows that the current response of the MGCE increases linearly while increasing the applied scan rate with  $R^2 = 0.973$ . This suggests that detection of serotonin on an MGCE surface involves the adsorption process compared to the diffusions process. The cyclic stability and repeatability of the electrochemical sensors are the most important and desirable features for practical purposes. It is important to check the cyclic repeatability and stability of the fabricated MGCE for detection of serotonin. Thus, we collected 50 consecutive CVs of the MGCE in 80  $\mu\text{M}$  serotonin in 0.1 M PBS (pH = 7.0) at a scan rate of 50 mV/s. The obtained CVs of the MGCE for serotonin detection are displayed in Figure 7.

The CVs results showed insignificant variation in the current response of the MGCE after 50 consecutive cycles. The 1st, 10th, 25th, and 50th CV cycles of MGCE in 80  $\mu\text{M}$  serotonin in 0.1 M PBS (pH = 7.0) at a scan rate of 50 mV/s have been displayed in Figure 7, which suggests excellent repeatability and cyclic stability of the MGCE up to 50 cycles, and it retained more than 91% of its initial performance in terms of current response. According to previous reports [13], it has been observed that the differential pulse voltammetry (DPV) method is a more effective and sensitive technique compared to CV. Thus, we have also obtained DPVs of BGCE and MGCE in the presence of 2  $\mu\text{M}$  serotonin at an applied scan rate of 50 mV/s in 0.1 M PBS of pH 7.0. The obtained DPVs of the BGCE and MGCE are presented in Figure 8.

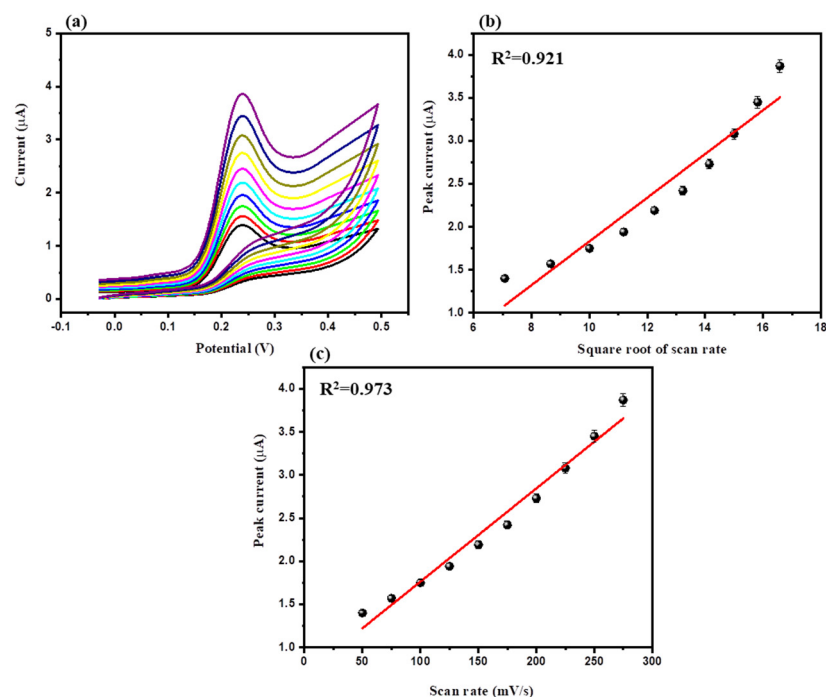


**Figure 6.** CVs (a) of MGCE in 2 μM serotonin in 0.1 M PBS (pH = 7.0) at various scan rates (50, 75, 100, 125, 150, 175, 200, 225, 250, and 275 mV/s). Calibration curve between peak current response versus square root of scan rate (b). Calibration curve between peak current response versus scan rate (c).

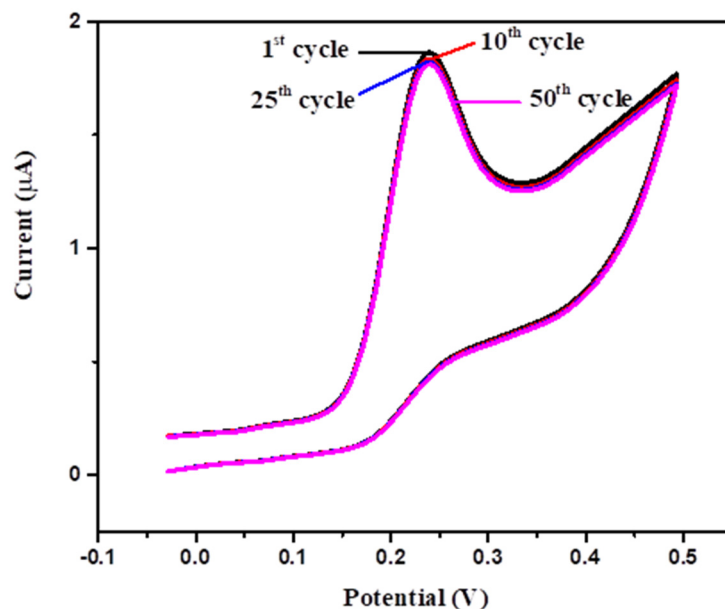


**Figure 7.** CVs of MGCE (1<sup>st</sup>, 10<sup>th</sup>, 25<sup>th</sup>, and 50<sup>th</sup> cycle) in 80 μM serotonin in 0.1 M PBS (pH = 7.0) at scan rate of 50 mV/s.

The BGCE shows a poor current response of 0.24 μA for detection of 2 μM serotonin in 0.1 M PBS (pH = 7.0) at a scan rate of 50 mV/s. The MGCE demonstrated an enhanced current response of 2.75 μA for detection of 2 μM serotonin in 0.1 M PBS (pH = 7.0) at a scan rate of 50 mV/s. Thus, MGCE has excellent electro-catalytic properties compared to BGCE, which may be due to the presence of α-MnO<sub>2</sub> in the fabricated MGCE. The DPVs investigations showed better electrochemical performance for MGCE compared to the CVs. The DPV current response of the MGCE was also recorded in absence of serotonin, and the

obtained results did not show any significant response (Figure 8). Thus, we have selected **MGCE** as the working electrode and DPV as an efficient detection technique for further electrochemical sensing studies. The above CVs showed that concentration of serotonin influences the electrochemical performance of **MGCE**. Thus, we have studied the effect of various concentrations (2  $\mu\text{M}$ , 6  $\mu\text{M}$ , 10  $\mu\text{M}$ , 14  $\mu\text{M}$ , 18  $\mu\text{M}$ , 22  $\mu\text{M}$ , 26  $\mu\text{M}$ , 30  $\mu\text{M}$ , 35  $\mu\text{M}$ , 40  $\mu\text{M}$ , 45  $\mu\text{M}$ , 50  $\mu\text{M}$ , 55  $\mu\text{M}$ , 60  $\mu\text{M}$ , 65  $\mu\text{M}$ , and 70  $\mu\text{M}$ ) of serotonin on the electrochemical activity of **MGCE** (0.1 M PBS of pH 7.0 (applied scan rate = 50 mV/s).

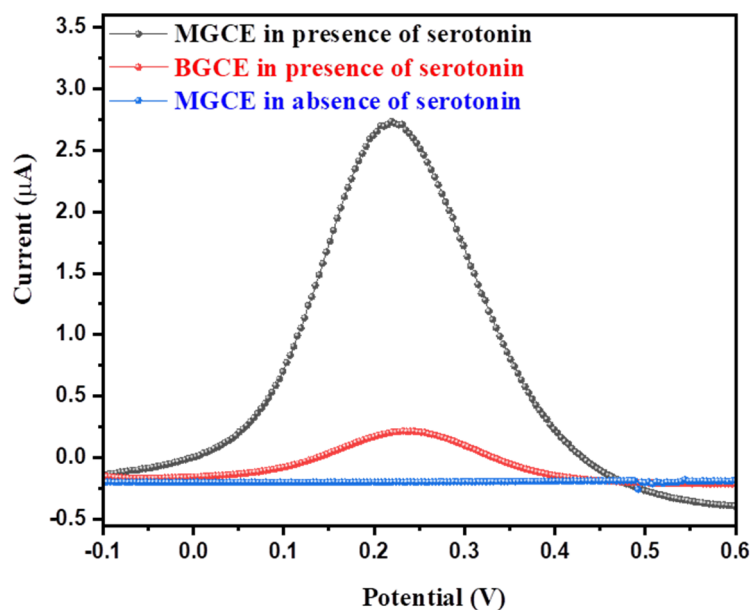


**Figure 8.** DPVs of BGCE and MGCE in absence and presence of 2  $\mu\text{M}$  serotonin in 0.1 M PBS (pH = 7.0) at scan rate of 50 mV/s.

The obtained DPVs of the **MGCE** in different concentrations of serotonin (2  $\mu\text{M}$ , 6  $\mu\text{M}$ , 10  $\mu\text{M}$ , 14  $\mu\text{M}$ , 18  $\mu\text{M}$ , 22  $\mu\text{M}$ , 26  $\mu\text{M}$ , 30  $\mu\text{M}$ , 35  $\mu\text{M}$ , 40  $\mu\text{M}$ , 45  $\mu\text{M}$ , 50  $\mu\text{M}$ , 55  $\mu\text{M}$ , 60  $\mu\text{M}$ , 65  $\mu\text{M}$ , and 70  $\mu\text{M}$ ) at a fixed scan rate of 50 mV/s (0.1 M PBS; PBS = 7.0) are summarized in Figure 9a. The DPVs show that current response increases with respect to concentration of serotonin. The calibration curve between current response versus concentration of serotonin is shown in Figure 9b. The polynomial fitted calibration curve between peak current response versus concentration of serotonin is presented in Figure S1.

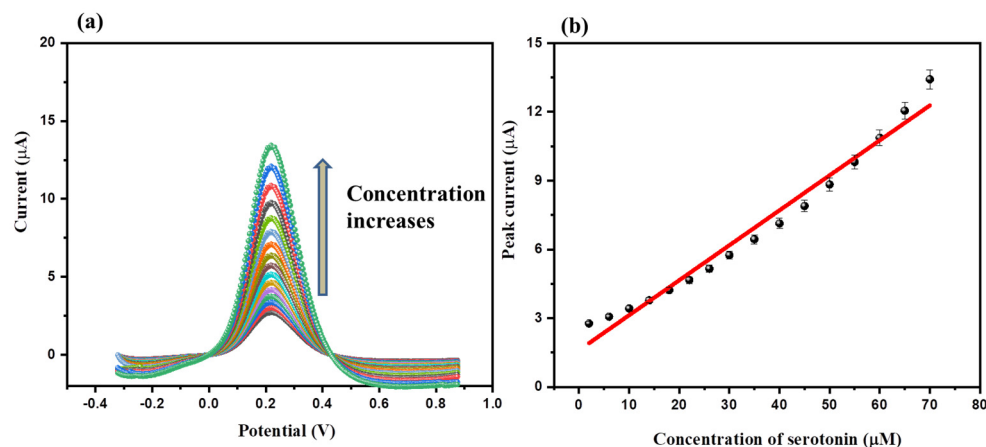


**Figure 9.** DPVs (a) of **MGCE** in various concentrations (2  $\mu\text{M}$ , 6  $\mu\text{M}$ , 10  $\mu\text{M}$ , 14  $\mu\text{M}$ , 18  $\mu\text{M}$ , 22  $\mu\text{M}$ , 26  $\mu\text{M}$ , 30  $\mu\text{M}$ , 35  $\mu\text{M}$ , 40  $\mu\text{M}$ , 45  $\mu\text{M}$ , 50  $\mu\text{M}$ , 55  $\mu\text{M}$ , 60  $\mu\text{M}$ , 65  $\mu\text{M}$ , and 70  $\mu\text{M}$ ) of serotonin in 0.1 M PBS (pH = 7.0) at scan rate of 50 mV/s. Calibration plot (b) between current response versus concentration of serotonin.

Selectivity of the electrochemical sensors is one of the most important desirable features for practical purposes. Thus, it is of great importance to examine the selectivity of the fabricated **MGCE**. The DPV graph of the **MGCE** was obtained in the presence of 20  $\mu\text{M}$  serotonin, and 20  $\mu\text{M}$  serotonin + interfering species (such as urea, hydroquinone, glucose, dopamine, ascorbic acid, etc.) were collected at a fixed scan rate of 50 mV/s (Figure 10). The concentration of interfering species was five times higher than that of the serotonin. All the interfering species were mixed with the 20  $\mu\text{M}$  serotonin solution. The observations suggest that the presence of interfering species could not significantly influence the electrochemical performance of **MGCE**. This indicates that **MGCE** has excellent selectivity for serotonin (Figure 10). The concentration of interfering species was higher than that of serotonin.

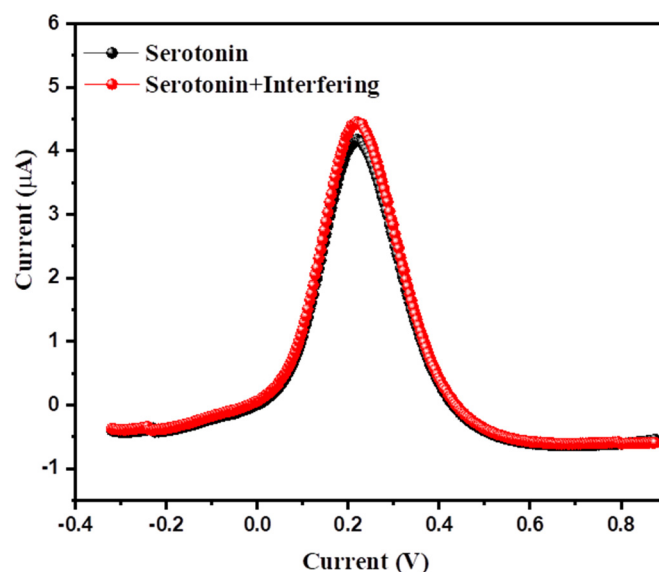


**Figure 10.** DPVs of **MGCE** in 20  $\mu\text{M}$  of serotonin and serotonin + interfering species (urea, glucose, dopamine, hydroquinone, ascorbic acid) in 0.1 M PBS (pH = 7.0) at scan rate of 50 mV/s.

Repeatability of the electrochemical sensor is another significant desirable characteristic. The repeatability of the **MGCE** was also investigated using DPV. The 50 consecutive DPV graphs of the **MGCE** were obtained in the presence of 20  $\mu\text{M}$  serotonin at a scan rate of 50 mV/s. The 1st, 10th, 25th, and 50th DPV graphs of the **MGCE** in the presence of 20  $\mu\text{M}$  serotonin in 0.1 M PBS (pH = 7.0) at a scan rate of 50 mV/s are presented in Figure 11.

There was insignificant variation/change observed, which suggests good repeatability and stability up to 50 cycles and revealed that **MGCE** retained ~89.7% of its initial performance in terms of current response. Reproducibility of the **MGCE** was also examined by fabricating four different **MGCEs**. The DPVs of the four freshly prepared **MGCEs** were obtained in 20  $\mu\text{M}$  of serotonin in 0.1 M PBS (pH = 7.0) at a scan rate of 50 mV/s. The obtained results are depicted in Figure S2 and showed good reproducibility.

The storage stability of the **MGCE** was also checked using DPV. The **MGCE** was stored for 10 days in a vacuum desiccator, and the DPV curve of the **MGCE** was recorded in the presence of 20  $\mu\text{M}$  serotonin in 0.1 M PBS of pH 7.0 at a scan rate of 50 mV/s, and the obtained results are compiled in Figure 12.

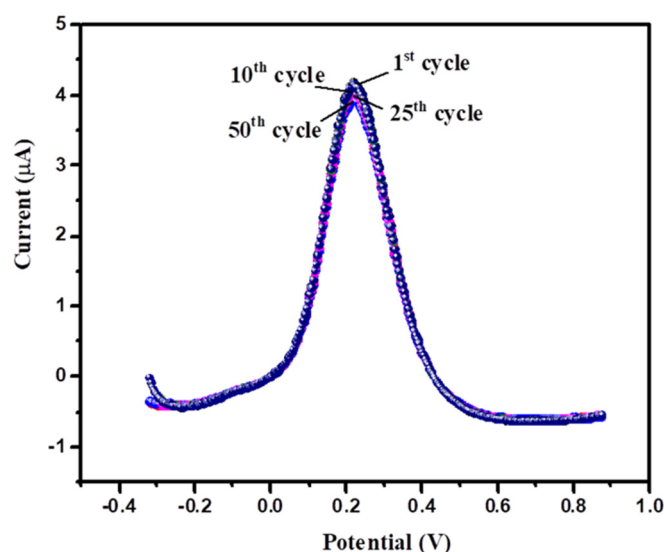


**Figure 11.** 1st, 10th, 25th, and 50th DPVs of MGCE in 20  $\mu\text{M}$  of serotonin in 0.1 M PBS (pH = 7.0) at scan rate of 50 mV/s.

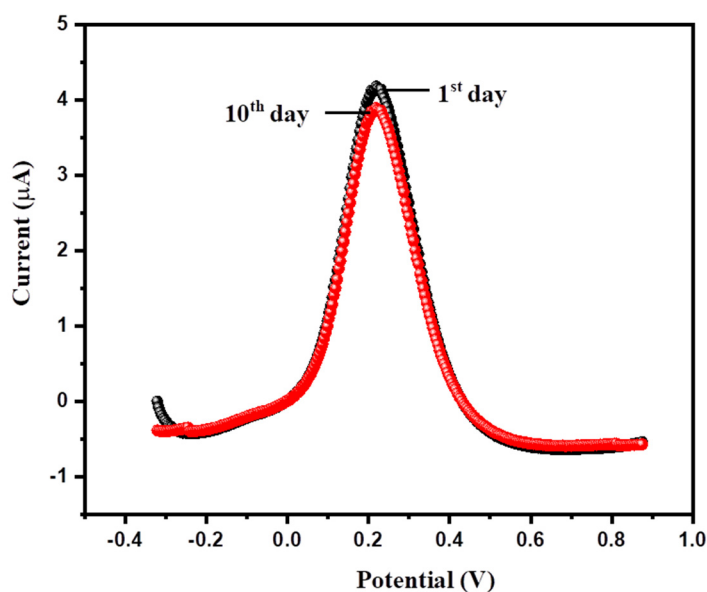


**Figure 12.** DPVs of MGCE (1st day and after 10th day) in 20  $\mu\text{M}$  of serotonin in 0.1 M PBS (pH = 7.0) at scan rate of 50 mV/s.

The obtained results suggest good storage stability after 10 days and retained more than 84% of the initial performance in terms of current response.

Real sample analysis was also conducted using the standard addition method. The 20  $\mu\text{M}$  of serotonin was added to the urine sample (collected from healthy person, male, age 29 years old), and the DPV curve was recorded as shown in Figure S3. The observations showed a good recovery of 98.4% using the standard addition method. Furthermore, we also investigated the selectivity of the MGCE in a urine sample. The DPV of the MGCE was recorded in the presence of 20  $\mu\text{M}$  serotonin + glucose, 20  $\mu\text{M}$  serotonin + urea, 20  $\mu\text{M}$  serotonin + ascorbic acid, 20  $\mu\text{M}$  serotonin + hydroquinone, and 20  $\mu\text{M}$  serotonin + dopamine at a scan rate of 50 mV/s (Figure S4). The concentration of interfering species was five times higher than that of serotonin. There was no significant change observed, which indicated good selective nature of MGCE for serotonin determination.

The probable mechanism for detection of serotonin has been illustrated in Scheme 2.

The electrochemical performance of the **MGCE** was evaluated by calculating detection limit (LoD) and sensitivity. The LoD and sensitivity of the **MGCE** were calculated using the following equations provided below:

$$\text{LoD} = \frac{3.3 * \sigma_b}{S} \quad (2)$$

(Herein,  $\sigma_b$  = standard deviation or error of the blank, and S = slope of the calibration curve).

$$\text{Sensitivity} = \frac{S}{A} \quad (3)$$

(where A = area of the electrode)

The **MGCE** exhibited an excellent LoD and sensitivity of 0.14  $\mu\text{M}$  and 2.41  $\mu\text{A } \mu\text{M}^{-1}\text{cm}^{-2}$ , respectively.

Over the past few years, various serotonin sensors were reported using nanostructured electrode materials. In this regard, Matt et al. [13] fabricated a  $\text{ZrO}_2$ -based serotonin sensor that showed a good LoD of 0.585  $\mu\text{M}$ . In other work, Babaei et al. [25] demonstrated the sensing behavior of Nafion/ $\text{Ni}(\text{OH})_2$ /multi-walled carbon nanotubes (MWCNTs)/GCE towards detection of serotonin and obtained an LoD of 0.083  $\mu\text{M}$ . Rand et al. [26] employed carbon nanofibers (CNFs) as a serotonin sensor and the authors reported an LoD of 0.25  $\mu\text{M}$ . In another report, Matuschek et al. [36] used a 3D mesoporous ITO electrode as a working electrode for detection of serotonin. This applied sensor exhibited an LoD of 7.5  $\mu\text{M}$  using the DPV method. Reddaiah et al. [37] designed and fabricated poly-Alizarin Red S/MWCNTs as electrode material for construction of a serotonin sensor. This prepared material (poly-Alizarin Red S/MWCNTs) was deposited on GCE, which demonstrated an excellent LoD of 0.18  $\mu\text{M}$ . Gupta et al. [38] also developed a serotonin sensor using novel strategies. The authors prepared polymelamine/pyrolytic graphite using a benign approach, and the working surface of GCE was modified with polymelamine/pyrolytic graphite as an electrode modifier. This fabricated electrode (polymelamine/pyrolytic graphite/GCE) exhibited a good LoD of 0.49  $\mu\text{M}$  for sensing of serotonin [38]. Citicoline-sodium-modified carbon paste electrode (CDP-Choline/MCPE) was also constructed by Deepa et al. [39] and employed as a serotonin sensor. This sensor showed an LoD of 5.81  $\mu\text{M}$ . In other work, Cernat et al. [40] fabricated a serotonin sensor using AuNPs@PPy/GSPE as a working electrode. This working electrode (AuNPs@PPy/GSPE)-based serotonin sensor exhibits an LoD of 32.22  $\mu\text{M}$  [40]. Mahanthesh et al. [41] also utilized a graphite pencil as a working electrode and employed a serotonin sensor that showed a decent LoD of 4  $\mu\text{M}$  [41]. Li et al. [42] prepared poly (basic red 9)-doped functionalized multi-walled carbon nanotubes and constructed a serotonin sensor. This serotonin sensor showed a good LoD of 9  $\mu\text{M}$  using poly (basic red 9)-doped functionalized multi-walled carbon nanotubes as an electrode modifier [42]. In 2019, Shahid et al. [43] also fabricated a serotonin sensor using reduced graphene oxide/cobalt oxide (rGO/ $\text{Co}_3\text{O}_4$ ) as an electrode-modifier. The authors fabricated GCE/rGO/ $\text{Co}_3\text{O}_4$  as a serotonin sensor, which displayed an LoD of 1.1  $\mu\text{M}$ . Another report based on nickel oxide/barium titanate ( $\text{NiO}/\text{BaTiO}_3$ ) also showed good performance for detection of serotonin [44]. Our obtained results for **MGCE** are comparable with previously reported sensors in terms of LoD, as listed in Table 1 [13,25,26,36–44].

**Table 1.** Comparison of LoD and linear range of MGCE with previous reports [13,25,26,36–44].

Material	LoD ( $\mu\text{M}$ )	Linear Range ( $\mu\text{M}$ )	References
MGCE	0.14	2–80	Present study
ZrO <sub>2</sub>	0.585	10–50	13
Nafion/Ni(OH) <sub>2</sub> /MWNTs/GCE	0.083	0.15–14.2	25
Carbon nanofibers	0.25	1–10	26
3D mesoporous ITO electrode	7.5	50–1000	36
Poly-Alizarin Red S/MWCNTs/GCE	0.18	0.5–10	37
Polymelamine/pyrolytic graphite/GCE	0.49	1–100	38
Citicoline-sodium-modified carbon paste electrode	5.81	10–30	39
AuNPs@PPy/GSPE	32.22	0.1–30	40
GPE	4	40–750	41
F-MWCNTs/BR9	9	10–83	42
rGO/Co <sub>3</sub> O <sub>4</sub>	1.1	1–10	43
NiO/BaTiO <sub>3</sub>	0.03	0.05–5	44

#### 4. Conclusions

In summary, we can conclude that nanorods of  $\alpha\text{-MnO}_2$  have been obtained using a hydrothermal method, which was characterized by various advanced characterization methods. Further, a glassy-carbon-electrode-based cost-effective serotonin sensor was developed. The developed serotonin sensor ( $\alpha\text{-MnO}_2/\text{GCE}$ ) showed excellent electrochemical performance for determination of serotonin in terms of sensitivity and detection limit using differential pulse voltammetry. In further investigations,  $\alpha\text{-MnO}_2/\text{GCE}$  also showed good repeatability, stability, and selectivity towards detection of serotonin.

**Supplementary Materials:** The following supporting information can be downloaded at: <https://www.mdpi.com/article/10.3390/bios12100849/s1>, Figure S1. Calibration curve between current response versus concentration of serotonin, Figure S2. DPVs of four freshly fabricated MGCE in 20  $\mu\text{M}$  of serotonin in 0.1 M PBS (pH=7.0) at scan rate of 50 mV/s, Figure S3. DPV of MGCE in 20  $\mu\text{M}$  of serotonin in urine at scan rate of 50 mV/s. Inset shows urine sample, Figure S4. DPVs of MGCE in 20  $\mu\text{M}$  of serotonin with different interfering species in urine at scan rate of 50 mV/s.

**Author Contributions:** Conceptualization, M.Q.K. and K.A.; Methodology, R.A.K., M.Q.K. and K.A.; Formal analysis, K.A., R.A.K. and M.Q.K.; Writing—original draft, M.Q.K., A.A. and K.A.; Writing—review & editing, H.K. and A.A.; Supervision, H.K. and A.A. Funding acquisition, H.K. and A.A. All authors have read and agreed to the published version of the manuscript.

**Funding:** This work was supported by the Korea Innovation Foundation (INNOPOLIS) grant funded by the Korea government (MSIT) (2020-DD-UP-0278) and the National Research Foundation of Korea (NRF) grant funded by the Korea government (MSIT) (No. 2019R1A5A8080290).

**Institutional Review Board Statement:** Not applicable.

**Informed Consent Statement:** Not applicable.

**Data Availability Statement:** Not applicable.

**Acknowledgments:** A.A. acknowledged researchers supporting project number (RSP-2021/78), King Saud University, Riyadh, Saudi Arabia.

**Conflicts of Interest:** The authors declare no conflict of interest.

#### References

1. Baranwal, A.; Chandra, P. Clinical implications and electrochemical biosensing of monoamine neurotransmitters in body fluids, in vitro, in vivo, and ex vivo models. *Biosens. Bioelectron.* **2018**, *121*, 137–152. [CrossRef] [PubMed]

2. Su, M.; Lan, H.; Tian, L.; Jiang, M.; Cao, X.; Zhu, C.; Yu, C. Ti<sub>3</sub>C<sub>2</sub>T<sub>x</sub>-reduced graphene oxide nanocomposite-based electrochemical sensor for serotonin in human biofluids. *Sens. Actuators B Chem.* **2022**, *367*, 132019. [[CrossRef](#)]
3. Khoshnevisan, K.; Maleki, H.; Honarvarfard, E.; Baharifar, H.; Gholami, M.; Faridbod, F.; Larijani, B.; Majidi, R.F.; Khorramizadeh, M.R. Nanomaterial based electrochemical sensing of the biomarker serotonin: A comprehensive review. *Microchim. Acta.* **2019**, *186*, 49. [[CrossRef](#)] [[PubMed](#)]
4. Ashraf, G.; Asif, M.; Aziz, A.; Iftikhar, T.; Liu, H. Rice-spikelet-like copper oxide decorated with platinum stranded in the CNT network for electrochemical in vitro detection of serotonin. *ACS Appl. Mater. Interfaces* **2021**, *13*, 6023–6033. [[CrossRef](#)]
5. Sharma, S.; Singh, N.; Tomar, V.; Chandra, R. A review on electrochemical detection of serotonin based on surface modified electrodes. *Biosens. Bioelectron.* **2018**, *107*, 76–93. [[CrossRef](#)]
6. Sha, Q.; Sun, B.; Yi, C.; Guan, R.; Fei, J.; Hu, Z.; Liu, B.; Liu, X. A fluorescence turn-on biosensor based on transferrin encapsulated gold nanoclusters for 5-hydroxytryptamine detection. *Sens. Actuators B Chem.* **2019**, *294*, 177–184. [[CrossRef](#)]
7. Tsuchiya, H.; Hayashi, T.; Tsumi, M.; Hoshino, Y.; Ohtani, S.; Takagi, N. High performance liquid-chromatographic analysis for serotonin and tryptamine excreted in urine after oral loading with L-tryptophan. *Clin. Chem.* **1989**, *35*, 43–47. [[CrossRef](#)]
8. Chauveau, J.; Fert, V.; Morel, A.M.; Delaage, M.A. Rapid and specific enzyme immunoassay of serotonin. *Clin. Chem.* **1991**, *37*, 1178–1184. [[CrossRef](#)]
9. Solinova, V.; Zakova, L.; Jiracek, J.; Kasicka, V. Pressure assisted partial filling affinity capillary electrophoresis employed for determination of binding constants of human insulin hexamer complexes with serotonin, dopamine, arginine, and phenol. *Anal. Chim. Acta* **2019**, *1052*, 170–178. [[CrossRef](#)]
10. Pradhan, T.; Jung, H.S.; Jang, J.H.; Kim, T.W.; Kang, C.; Kim, J.S. Chemical sensing of neurotransmitters. *Chem. Soc. Rev.* **2014**, *43*, 4684–4713. [[CrossRef](#)]
11. Amatongchai, M.; Sitanurak, J.; Sroysee, W.; Sodanath, S.; Chairam, S.; Jarujamrus, P.; Nacapricha, D.; Lieberzeit, P.A. Highly sensitive and selective electrochemical paper-based device using a graphite screen-printed electrode modified with molecularly imprinted polymers coated Fe<sub>3</sub>O<sub>4</sub>@Au@SiO<sub>2</sub> for serotonin determination. *Anal. Chim. Acta* **2019**, *1077*, 255–265. [[CrossRef](#)] [[PubMed](#)]
12. Wolrab, D.; Frühauf, P.; Gerner, C. Quantification of the neurotransmitters melatonin and N-acetyl-serotonin in human serum by supercritical fluid chromatography coupled with tandem mass spectrometry. *Anal. Chim. Acta* **2016**, *937*, 168–174. [[CrossRef](#)] [[PubMed](#)]
13. Matt, S.B.; Shivanna, M.; Manjunath, S.; Siddalinganahalli, M.; Siddalingappa, D.M. Electrochemical detection of serotonin using t-ZrO<sub>2</sub> nanoparticles modified carbon paste electrode. *J. Electrochem. Soc.* **2020**, *167*, 155512. [[CrossRef](#)]
14. Khoshnevisan, K.; Baharifar, H.; Torabi, F.; Afjeh, F.S.; Maleki, H.; Honarvarfard, E.; Mohammadi, H.; Sajjadi-Jazi, S.M.; Mahmoudi-Kohan, S.; Faridbod, F.; et al. Serotonin level as a potent diabetes biomarker based on electrochemical sensing: A new approach in a zebra fish model. *Anal. Bioanal. Chem.* **2021**, *413*, 1615–1627. [[CrossRef](#)]
15. Ahmad, K.; Kumar, P.; Mobin, S.N. A highly sensitive and selective hydroquinone sensor based on a newly designed N-rGO/SrZrO<sub>3</sub> composite. *Nanoscale Adv.* **2020**, *2*, 502–511. [[CrossRef](#)] [[PubMed](#)]
16. Ahmad, K.; Kumar, P.; Mobin, S.M. Hydrothermally Grown SnO<sub>2</sub> Flowers as Efficient Electrode Modifier for Simultaneous Detection of Catechol and Hydroquinone. *J. Electrochem. Soc.* **2019**, *166*, B1577. [[CrossRef](#)]
17. Ahmad, K.; Mobin, S.M. Shape controlled synthesis of high surface area MgO microstructures for highly efficient congo red dye removal and peroxide sensor. *J. Environ. Chem. Eng.* **2019**, *7*, 103347. [[CrossRef](#)]
18. Ahmad, K.; Kumar, P.; Mobin, S.M. Hydrothermally grown novel pyramids of the CaTiO<sub>3</sub> perovskite as an efficient electrode modifier for sensing applications. *Mater. Adv.* **2020**, *1*, 2003–2009. [[CrossRef](#)]
19. Ahmad, K.; Mobin, S.M. High surface area 3D-MgO flowers as the modifier for the working electrode for efficient detection of 4-chlorophenol. *Nanoscale Adv.* **2019**, *1*, 719–727. [[CrossRef](#)]
20. Anithaa, A.C.; Asokan, K.; Sekar, C. Highly sensitive and selective serotonin sensor based on gamma ray irradiated tungsten trioxide nanoparticles. *Sens. Actuators B* **2017**, *238*, 667–675. [[CrossRef](#)]
21. Wei, X.; Wang, F.; Yin, Y.; Liu, Q.; Zou, L.; Ye, B. Selective detection of neurotransmitter serotonin by a gold nanoparticles-modified glassy carbon electrode. *Analyst* **2010**, *135*, 2286–2290. [[CrossRef](#)] [[PubMed](#)]
22. Abbaspour, A.; Noori, A. A cyclodextrin host-guest recognition approach to an electrochemical sensor for simultaneous quantification of serotonin and dopamine. *Biosens. Bioelectron.* **2011**, *26*, 4674–4680. [[CrossRef](#)] [[PubMed](#)]
23. Xue, C.; Wang, X.; Zhu, W.; Han, Q.; Zhu, C.; Hong, J.; Zhou, X.; Jiang, H. Electrochemical serotonin sensing interface based on double-layered membrane of reduced graphene oxide/polyaniline nanocomposites and molecularly imprinted polymers embedded with gold nanoparticles. *Sens. Actuators B* **2014**, *196*, 57–63. [[CrossRef](#)]
24. Wang, F.; Wu, Y.; Lu, K.; Ye, B. A simple but highly sensitive and selective calixarene-based voltammetric sensor for serotonin. *Electrochim. Acta* **2013**, *87*, 756–762. [[CrossRef](#)]
25. Babaei, A.; Taheri, A.R. Nafion/Ni(OH)<sub>2</sub> nanoparticles-carbon nanotube composite modified glassy carbon electrode as a sensor for simultaneous determination of dopamine and serotonin in the presence of ascorbic acid. *Sens. Actuators B* **2013**, *176*, 543–551. [[CrossRef](#)]
26. Rand, E.; Periyakaruppan, A.; Tanaka, Z.; Zhang, D.A.; Marsh, M.P.; Andrews, R.J.; Lee, K.H.; Chen, B.; Meyyappan, M.; Koehne, J.E. A carbon nanofiber based biosensor for simultaneous detection of dopamine and serotonin in the presence of ascorbic acid. *Biosens. Bioelectron.* **2013**, *42*, 434–438. [[CrossRef](#)]

27. Kim, S.K.; Kim, D.; Jeon, S. Electrochemical determination of serotonin on glassy carbon electrode modified with various graphene nanomaterials. *Sens. Actuators B* **2012**, *174*, 285–291. [[CrossRef](#)]
28. Wu, B.; Yeasmin, S.; Liu, Y.; Cheng, L.-J. Sensitive and selective electrochemical sensor for serotonin detection based on ferrocene-gold nanoparticles decorated multiwall carbon nanotubes. *Sens. Actuators B Chem.* **2022**, *354*, 131216. [[CrossRef](#)]
29. Prathap, M.U.A.; Sun, S.; Xu, Z.J. An electrochemical sensor highly selective for lindane determination: A comparative study using three different  $\alpha$ -MnO<sub>2</sub> nanostructures. *RSC Adv.* **2016**, *6*, 22973–22979. [[CrossRef](#)]
30. Sohal, N.; Maity, B.; Shetti, N.P.; Basu, S. Biosensors Based on MnO<sub>2</sub> Nanostructures: A Review. *ACS Appl. Nano Mater.* **2021**, *4*, 2285–2302. [[CrossRef](#)]
31. Ahmad, K.; Mohammad, A.; Mobin, S.M. Hydrothermally grown  $\alpha$ -MnO<sub>2</sub> nanorods as highly efficient low cost counter-electrode material for dye-sensitized solar cells and electrochemical sensing applications. *Electrochim. Acta* **2017**, *252*, 549–557. [[CrossRef](#)]
32. Zhao, G.-y.; Wang, F.-c.; Liu, M.-j.; Sui, Y.-m.; Zhang, Z.; Kang, F.-y.; Yang, C. A high-frequency flexible symmetric supercapacitor prepared by the laser-defocused ablation of MnO<sub>2</sub> on a carbon cloth. *New Carbon Mater.* **2022**, *37*, 556–563. [[CrossRef](#)]
33. Boyom-Tatchemo, F.W.; Devred, F.; Ndiffo-Yemeli, G.; Laminsi, S.; Gaigneaux, E.M. Plasma-induced redox reactions synthesis of nanosized  $\alpha$ -,  $\gamma$ - and  $\delta$ -MnO<sub>2</sub> catalysts for dye degradation. *Appl. Catal. B Environ.* **2020**, *260*, 118159. [[CrossRef](#)]
34. Deng, P.; Fang, H.; Liu, R.; Guo, X.; Chen, P. One-pot hydrothermal synthesis of flower-like MnO<sub>2</sub> nanostructure with rich oxygen vacancy for catalysis thermal-induced pyrolysis of energetic molecular perovskite. *Vacuum* **2022**, *203*, 111234. [[CrossRef](#)]
35. Liu, Z.; Yang, Y.; Lu, B.; Liang, S.; Fan, H.J.; Zhou, J. Insights into complexing effects in acetate-based Zn-MnO<sub>2</sub> batteries and performance enhancement by all-round strategies. *Energy Storage Mater.* **2022**, *52*, 104–110. [[CrossRef](#)]
36. Matuschek, L.; Gobel, G.; Lisdat, F. Electrochemical detection of serotonin in the presence of 5-hydroxyindoleacetic acid and ascorbic acid by use of 3D ITO electrodes. *Electrochem. Commun.* **2017**, *81*, 145–149. [[CrossRef](#)]
37. Reddaiah, K.; Rao, K.S.V.K.; Reddy, T.M. Electrochemical Detection of Serotonin in Human Serum Sample and Simultaneous Resolution in Presence of Epinephrine. *Anal. Bioanal. Electrochem.* **2018**, *10*, 175–191.
38. Gupta, P.; Goyal, R.N. Polymelamine modified edge plane pyrolytic graphite sensor for the electrochemical assay of serotonin. *Talanta* **2014**, *120*, 17–22. [[CrossRef](#)]
39. Deepa, S.; Swamy, B.E.K.; Pai, K.V. Electrochemical sensing performance of citicoline sodium modified carbon paste electrode for determination of dopamine and serotonin. *Mater. Sci. Energy Technol.* **2020**, *3*, 584–592. [[CrossRef](#)]
40. Cernat, M.T.A.; Florea, D.L.A.; Bogdan, D.; Suci, M.; Sandulescu, R.; Cristea, C. Highly selective electrochemical detection of serotonin on polypyrrole and gold nanoparticles-based 3D architecture. *Electrochem. Commun.* **2017**, *75*, 43–47.
41. Mahanthesh, K.R.; Swamy, B.E.K.; Chandra, U. Simultaneous determination of dopamine in presence of serotonin at a graphite pencil electrode: A voltammetric study. *Anal. Bioanal. Electrochem.* **2018**, *10*, 1064–1079.
42. Li, Y.; Ali, M.A.; Chen, S.-M.; Yang, S.-Y.; Lou, B.-S.; Al-Hemaid, F.M.A. Poly(basic red 9) doped functionalized multiwalled carbon nano-tubes as composite films for neurotransmitters biosensors. *Colloids Surf. B Biointerfaces* **2014**, *118*, 133–139. [[CrossRef](#)] [[PubMed](#)]
43. Shahid, M.M.; Ramesh Kumar, P.; Numan, A.; Shahabuddin, S.; Alizadeh, M.; Khiew, P.S.; Chiu, W.S. A cobalt oxide nanocubes interleaved reduced graphene oxide nanocomposite modified glassy carbon electrode for amperometric detection of serotonin. *Mater. Sci. Eng. C* **2019**, *100*, 388–395. [[CrossRef](#)] [[PubMed](#)]
44. Ran, G.; Xia, Y.; Zhang, H.; Kuang, W.; Fu, C. An atomic-layer NiO-BaTiO<sub>3</sub> nanocomposite for use in electrochemical sensing of serotonin. *Nanotechnology* **2020**, *31*, 505502. [[CrossRef](#)] [[PubMed](#)]